Uturnitin Originality Report

<u>from palm-based biodiesel</u> by Shella Santoso	Similarity Index	Internet Sources: Publications: Student Papers:	N/A 20% N/A
From Similarity Check (check paper Jakad SPS)			
Processed on 28-Feb-2022 15:36 WIB ID: 1772792969			
Word Count: 7371	ources:		
waste capiz shell - based catalyst for the conv of Environmental Chemical Engineering, 2020	Edi Soetaredjo, Su version of leather tanning	<u>lla Permatasari Santo</u> ryadi Ismadji et al. "U	tilization o
2 1% match (publications) Duangkamol Na-Ranong, Pattarin Laur glucosides in palm oil based biodiesel u 2015			
3 1% match (publications) <u>Maria Yuliana, Luciana Trisna, Feprita S</u> <u>PURIFICATION USING REACTIVATED</u> <u>REFINERIES: ZERO-WASTE APPROACH", .</u>	<u>) SPENT BLEACHING I</u>	EARTH FROM PALM	
4 1% match (publications) <u>Maria Yuliana, Shella Permatasari Santone-pot synthesis of biodiesel from leatont optimization", Biomass and Bioenergy, 2020</u>			
5 1% match (publications) Jenni Lie, Maria Bangun Rizkiana, Fely Yuliana. "Non-catalytic Transesterificati Content Using Subcritical Methanol: Process of Valorization, 2019	on of Waste Cooking O	I with High Free Fatty	<u>/ Acids</u>
6 1% match (publications)			
Maria Yuliana, Suryadi Ismadji, Jenni L structured alginate-immobilized benton antibiotics from aqueous solution", Environme	<u>ite beads designed for a</u>		
Maria Yuliana, Suryadi Ismadji, Jenni L structured alginate-immobilized benton	ite beads designed for a ntal Research, 2022 cky Mulyono, Shella Per ble-shelled hollow meso	n effective removal c matasari Santoso, M oporous silica as acid	<u>f persister</u> aria -base

1% match (publications)

Rishi Rathour, Papita Das, Kaustav Aikat. "Microwave-assisted synthesis of graphene and its application for adsorptive removal of malachite green: thermodynamics, kinetics and isotherm study", Desalination and Water Treatment, 2015

1% match (publications)

<u>Alexandre H. Pinto, Jeffrey K. Taylor, Richard Chandradat, Edmond Lam et al. "Wood-based</u> <u>cellulose nanocrystals as adsorbent of cationic toxic dye, Auramine O, for water treatment",</u> Journal of Environmental Chemical Engineering, 2020

1% match (publications)

"Green Adsorbents for Pollutant Removal", Springer Science and Business Media LLC, 2018



11

9

10

1% match (publications)

You Wei Chen, Hwei Voon Lee, Joon Ching Juan, Siew-Moi Phang. "Production of new cellulose nanomaterial from red algae marine biomass Gelidium elegans", Carbohydrate Polymers, 2016



< 1% match (publications)

Florencia Eberhardt, Andres Aguirre, Luciana Paoletti, Guillermo Hails et al. "Pilot-scale process development for low-cost production of a thermostable biodiesel refining enzyme in Escherichia coli", Bioprocess and Biosystems Engineering, 2018



< 1% match (publications)

Xu Hu, Jinhao Sun, Xing Li, Lijun Qian, Juan Li. " Effect of compound on flame retardancy and mechanical properties of polylactic acid ", Journal of Applied Polymer Science, 2020



< 1% match (publications)

<u>Caryn Hui Chuin Tan, Sumiyyah Sabar, M. Hazwan Hussin. "Development of immobilized</u> <u>microcrystalline cellulose as an effective adsorbent for methylene blue dye removal", South</u> <u>African Journal of Chemical Engineering, 2018</u>



17

18

19

< 1% match (publications)

<u>Ying Yang. "Some properties of polyphenol oxidase from lily", International Journal of Food</u> <u>Science & Technology, 01/2008</u>

< 1% match (publications)

Papita Saha, Shamik Chowdhury, Suyash Gupta, Indresh Kumar. "Insight into adsorption equilibrium, kinetics and thermodynamics of Malachite Green onto clayey soil of Indian origin", Chemical Engineering Journal, 2010

< 1% match (publications)

Sadanand Pandey. "A comprehensive review on recent developments in bentonite-based materials used as adsorbents for wastewater treatment", Journal of Molecular Liquids, 2017

< 1% match (publications)

Likozar, Blaž, Andrej Pohar, and Janez Levec. "Transesterification of oil to biodiesel in a continuous tubular reactor with static mixers: Modelling reaction kinetics, mass transfer, scaleup and optimization considering fatty acid composition", Fuel Processing Technology, 2016.



21

< 1% match (publications)

Huali Wang. "Analysis of Sterol Glycosides in Biodiesel and Biodiesel Precipitates", Journal of the American Oil Chemists' Society, 10/29/2009

< 1% match (publications)

Yang Hu, Lirong Tang, Qilin Lu, Sigun Wang, Xuerong Chen, Biao Huang, "Preparation of cellulose nanocrystals and carboxylated cellulose nanocrystals from borer powder of bamboo". Cellulose, 2014

22

< 1% match (publications)

Shamik Chowdhury, Papita Das (Saha). "Mechanistic, Kinetic, and Thermodynamic Evaluation of Adsorption of Hazardous Malachite Green onto Conch Shell Powder", Separation Science and Technology, 2011

< 1% match (publications)

23 Yujia Liu, Danyang Ying, Luz Sanguansri, Yanxue Cai, Xueyi Le. "Adsorption of catechin onto cellulose and its mechanism study: Kinetic models, characterization and molecular simulation", Food Research International, 2018

< 1% match (publications)

G. León, F. García, B. Miguel, J. Bayo. "Equilibrium, kinetic and thermodynamic studies of methyl orange removal by adsorption onto granular activated carbon", Desalination and Water Treatment, 2015



26

24

< 1% match (publications)

Norasikin Saman, Khairiraihanna Johari, Shiow-Tien Song, Helen Kong, Siew-Chin Cheu, Hanapi Mat. "High removal efficacy of Hg(II) and MeHg(II) ions from aqueous solution by organoalkoxysilane-grafted lignocellulosic waste biomass", Chemosphere, 2017

< 1% match (publications)

Naba Kumar Mondal, Kousik Das, Biswajit Das, Bikash Sadhukhan. "Effective utilization of calcareous soil towards the removal of methylene blue from aqueous solution", Clean Technologies and Environmental Policy, 2015



28

< 1% match (publications)

Zhang, M.: "Fractionating lignocellulose by formic acid: Characterization of major components", Biomass and Bioenergy, 201004

< 1% match (publications)

Antonius Nova Rahadi, Jeremia Jonathan Martinus, Shella Permatasari Santoso, Maria Yuliana et al. " hollow mesoporous silica incorporated copper (II) (Cu/) as a catalyst to promote esterification/transesterification of palm oil ", International Journal of Energy Research, 2021



< 1% match (publications)

Sagnik Chakraborty, Shamik Chowdhury, Papita Das Saha. " Batch Removal of Crystal Violet from Aqueous Solution by H SO Modified Sugarcane Bagasse: Equilibrium, Kinetic, and Thermodynamic Profile ", Separation Science and Technology, 2012

paper text:

Renewable Energy 154 (2020) 99e106 Contents lists available at ScienceDirect Renewable Energy journal homepage: www.elsevier.com/locate/renene

1Feasibility study of nanocrystalline cellulose as adsorbent of steryl glucosides from palm-based biodiesel

Liangna Widdyaningsih a, 1, Albert Setiawan a, 1,

4**Shella Permatasari Santoso a, b, Felycia Edi Soetaredjo a, b, Suryadi Ismadji a, b**, Sandy Budi Hartono **a**, Yi-Hsu Ju **b, c**

, d, Phuong Lan Tran-Nguyen e, Maria Yuliana a, * a Department of Chemical Engineering, Widya Mandala Catholic University Surabaya, Kalijudan 37, Surabaya, 60114, Indonesia b Department of Chemical Engineering, National Taiwan University of Science and Technology, 43 Keelung Road, Sec 4, Taipei, 10607, Taiwan

1c Graduate Institute of Applied Science and Technology

1National Taiwan University of Science and Technology, 43 Keelung Road, Sec 4, Taipei, 10607, Taiwan d Taiwan Building Technology Center, National Taiwan University of Science and Technology, 43 Keelung Road, Sec 4, Taipei, 10607, Taiwan e Department of Mechanical Engineering, Can Tho University, 3-2 Street, Can Tho City, Viet Nam

article info Article history: Received 16 October 2019 Received in revised form 3 February 2020 Accepted 1 March 2020 Available online 4 March 2020 Keywords: Biodiesel Steryl glucosides removal Nanocrystalline cellulose Adsorption isotherm Adsorption mechanism Feasibility study abstract Increasing the content of biodiesel in the diesel fuel mixture faces some challenges

13due to the presence of steryl glucosides (SG) compounds, which

causes the filter clogging and the reduction of engine power. In this study, coarse filter paper-based nanocrystalline cellulose (CFP-based NCC) with the crystallinity of 85.73% is selected as a potential adsorbent to separate SG compounds in palm-based biodiesel (PO eB100). The adsorption experiments were carried out at various CFP-based NCC to PO-B100 mass ratio (1:50, 1:75, 1:100, 1:125, 1:150, 1:175, 1:200) and temperature (65, 75, 85 C). The maximum SG removal was 91.81%, obtained at 75 C for CFP-based NCC to PO-B100 mass ratio of 1:50. The adsorption treat- ment also improves the cold stability of PO-B100 by reducing the cloud point from 13.2 C to 11.5 C. Langmuir isotherm model is best-fitted to the equilibrium adsorption data

3and thermodynamic studies suggested that the adsorption of SG onto the

18surface is spontaneous and endothermic. The

isotherm and

18thermodynamic study showed that the mechanism governing the adsorption process

may be driven by both dipole-dipole interactions and ion exchange. The adsorption results showed that CFP-based NCC has great affinity and selectivity to SG and can be considered as a promising adsorbent of SG. © 2020 Elsevier Ltd. All rights reserved. 1. Introduction To date, petroleum diesel is used worldwide for transportation, manufacturing, power generation, construction and farming in- dustries. However, disruption in crude market price and the long- term availability along with the nature deterioration due to its gas emission have become the major concerns for environmental sustainability [1]. Therefore, it is necessary to develop alternative fuels that are environmentally friendly, especially as a substitute for diesel fuel. Of the several alternative fuels available, biodiesel is an alter- native diesel fuel made from renewable biological resources [2]. * Corresponding author. E-mail address: mariayuliana@ukwms.ac.id (M. Yuliana).

71 These authors contributed equally to this work

. https://doi.org/10.1016/j.renene.2020.03.001 0960-1481/© 2020 Elsevier Ltd. All rights reserved. Biodiesel is generally derived from transesterification of agricul- tural or animal lipids and

20short-chain alcohols in the presence of a catalyst

. Conventional base-catalyzed transesterification in a batch stirred-tank reactor is the most common technique used to produce the commercially available biodiesel [3]. Several modifications on the conversion route as well as the reactor configuration and design have been performed

19in order to create, optimize and intensify the continuous production of biodiesel

. The transesterification using catalyst-free subcritical [4e6] or supercritical alcohol [7,8], as well as heterogeneous [9] or enzymatic catalyst [9,10], gain wide attention in improving the continuity of biodiesel production. Likozar et al. (2016) also introduced

19a simple and robust design of a tubular reactor with a static

mixer to intensify the mass transfer rate between the reactants and increase the biodiesel conversion rate. Their work also studied the chemical equilibrium and reaction kinetics at different operating parameters to optimize the product Abbreviation SG MG DG TG CFP NCC FAME PO-B100 Steryl glucoside(s) Monoacylglyceride(s) Diacylglyceride(s) Triacylglyceride(s) Coarse filter paper Nanocrystalline cellulose Fatty Acid Methyl Ester(s) Palm-based biodiesel yield [11]. While biodiesel is currently mass-produced and a large number of studies have been carried out to improve its performance in various aspects, the white precipitates are still a challenge for its manufacturers. Although biodiesel distributed around the country must conform to the fuel property specifications as controlled by ASTM D6751, white precipitates were often detected in biodiesel and its blends during storage [12]. Several cases even showed that suspended particles in biodiesel have been found shortly after the production and at a rather high temperature (slightly below 60 C) [13]. The white precipitates may cause filter plugging in engine systems [13,14]. This phenomenon was also observed in many biodiesel plants and hence frequent maintenance and process modification are often essential to maintain plant effectiveness and efficiency.

13The presence of steryl glucosides (SG), which

is one of the plant sterols, has

13been identified as the major component of

the white precipitates. It mostly presents in biodiesel with a concentration of 35 ppm or higher [15]. The existence of this dispersed particles of SG promotes the aggregation of other components in biodiesel, saturated monoacylglycerides (MG) and diacylglycerides (DG), and subsequently affects the cold flow stability of fuel and widespread use [16]. Several techniques have been conducted to minimize the SG content in the biodiesel product, namely enzymatic hydrolysis [17,18], adsorption using magnesium silicate and bleaching earth [16] and ultrafiltration [19]. SG removal by enzymatic hydrolysis resulted in 81% removal efficiency with the addition of

13a synthetic codon-optimized version of the LacS gene

expressed from E. coli with the total operating time of 7 h [17]. Na-Ranong et al. (2015) reported that the conventional adsorption using magnesium sili- cate and bleaching earth in temperature of 65e80 C yielded in 81.4e82.5% removal efficiency of SG [16]. Tremblay and Montpetit (2017) stated that the highest separation for SG (86%) by ultrafil- tration was obtained when the biodiesel was transesterified using 0.7% (w/w) catalyst and 4:1 methanol:soybean oil molar ratio [19]. Based on the removal efficiency and economic feasibility, the adsorption treatment is a potential method to reduce SG content as well as to improve the cold flow properties of the fuel in the in- dustrial scale because it is found to be effective and facile, time-saving and energy-efficient. The development of adsorbent for effective adsorption has been conducted using various types of materials. Currently, the devel- opment of cellulosic adsorbent received major interest because it

11 is renewable, biodegradable, low cost, and non-toxic

[20].

11Cellulosic adsorbents have the ability to meet the requirement of being

a biosorbent, as it is abundantly available as a natural biopolymer. Cellulose in the form of nanocrystalline cellulose (NCC)

11has been widely studied due to its extensive industrial application, namely enzyme immobilization, adsorption, catalysis, drug delivery, bio- sensors and bio-imaging

[21]. NCC, with a large

11specific surface area and plenty of surface

hydroxyl and anionic sulfate ester group for physical and chemical reactions [22e24],

18can be considered as a new promising adsorbent for SG removal

. As the Indonesian government plans to increase the

7use of biodiesel in diesel blend from B20 to B30

in the time span of 5 years, the use of NCC for SG removal and improvement of the cold stability

1 is an interesting topic to be studied. The objective of this study is to observe the feasibility of

coarse filter paper-based NCC (CFP-based NCC) as the adsorption agent for SG. Various operating parameters, namely temperature, and the mass ratio of CFP-based NCC to palm- based biodiesel (POeB100) will be monitored. The adsorption mechanism was also proposed based on the isotherm and ther- modynamics study.

12. Materials and methods 2.1. Materials PO-B100 was collected from a local palm oil manufacturer in Gresik, Indonesia, and

stored for 3 days at room temperature prior to the adsorption experiment. Coarse filter paper (CFP) as the cellulosic material

6was obtained from a local supplier in Surabaya, Indonesia

. Sulphuric acid, sodium hydroxide, ethyl acetate, and

5n- hexane were purchased from Merck, Germany. FAMEs standard 47885 U contains 37 components FAME mix

7procured from Supelco (Bellefonte, PA, USA

) and Matreya (State College,

5PA, USA), respectively. Nitrogen gas (99.9% purity) was purchased from Aneka Gas Industry Pty. Ltd., Surabaya. All reagents were of analytical grade and required no further purification

. 2.2. Preparation of NCC CFP was ground into fibrous powder before use. The non- cellulosic material of CFP was subsequently removed to obtain purified cellulose using the modified method of Putro et al. (2017) [25]: 12 g of the CFP powder was delignified using 0.1 g/ml sodium hydroxide aqueous solution (40 ml). The delignified product was washed with distilled water and filtrated three times through a Whatman 1 (11 mm pore size) filter paper before being dried under vacuum at 80 C for 12 h. CFP-based NCC was prepared by using acid hydrolysis following the procedure conducted by Putro et al. (2017) [25]. 1 g of delignified cellulose was hydrolyzed with 20 ml sulphuric acid 64% at 45 C for 75 min under constant agitation. The reaction time was selected to ensure high reaction efficiency. After the specified duration, the reaction was immediately quenched using 20-fold of cold distilled water. The suspension

3was centrifuged at 4500 rpm for 10 min to remove the excess acid solution. The

resulting pre- cipitates were dialyzed against distilled water until neutral pH was achieved. The colloidal suspension was subjected to sonication treatment for 30 min in a cooling bath to avoid overheating and subsequently subjected to vacuum drying at 80 C for 6 h to obtain CFP-based NCC powder. 2.3.

1Characterization of CFP-based NCC The surface morphologies of

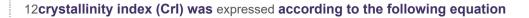
the CFP-based NCC particles were analyzed on a field emission scanning electron microscope (

1FESEM) JEOL JSM-6500F (Jeol Ltd., Japan), with an accelerating voltage of 5e10 kV and

9.5e9.6 mm working distance. The CFP-based NCC powder was attached to a stub, sputtered and coated with gold prior to analysis. Fourier Transform Infrared (FTIR) analysis was performed by an FTIR-8400S spectrophotometer (Shimadzu, Japan) in the range of 400e4000 cm?1 at a 4 cm?1 scanning resolution. L. Widdyaningsih et al. / Renewable Energy 154 (2020) 99e106 101 XRD analysis was conducted by

1an X'PERT Panalytical Pro X-Ray diffractometer (Philips-FEI, Netherlands) with monochromatic Cu Ka1 radiation at wavelength (I) ½ 0.154 nm, 40 kV of voltage and 30 mA of tube current. The

diffraction pattern was acquired in the range of 5 e60 (2q angle). The



, as proposed by Segal et al. (1959) [26]. Crl ð%Þ ¼ ðl200 ? lamÞ x100 (1) l200

. The crystallite size (nm) was calculated using the Scherrer analysis. 2.4. Compositional study of SG in PO-B100 using GC-FID analysis The analysis of SG composition in PO-B100

1was carried out using GC-17A (Shimadzu, Japan), completely equipped with a split/splitless injector and a flame ionization detector (FID). The separation was performed using nonpolar capillary column DB

- 5HT (5 %-phenyl)-methylpolysiloxane (15 m 0.32 mm ID, Agi- lent

1Technology, CA). The column temperature was initially set

at 80 C, then subsequently ramped to 365 C at the rate of 15 C/ min, and held constant for 19

1min. The temperature of the injector and detector were adjusted constant at 370 C

4100 mg of SG was dissolved in 1 ml

ethyl acetate

1and subjected to filtration using polyvinylidene difluoride (PVDF) filter prior analysis. The prepared sample (1 ml) was injected into the GC with a split ratio of 1:50. The velocity of nitrogen (N2, 99.9%) as the carrier gas was fixed at 30 cm/s at 80 C

. 2.5. Removal of SG using adsorption The adsorption of SG from PO-B100 was conducted in a batch mode according to the study conducted by Na-Ranong et al. (2015) with a few modifications [16]. A various mass ratio of CFP-based NCC to PO-B100 (1:50, 1:75, 1:100, 1:125, 1:150, 1:175, 1:200) was introduced into a series of beakers, where the mixture will be

3subjected to a 1-h adsorption process at constant temperature and agitation speed (250 rpm). The selection of adsorption duration was based on the preliminary experiment conducted to find the equi- librium time. Several adsorption temperatures (65, 75 and 85

3C) were used to study the effect of temperature on the adsorption of

SG. The solution was separated from the adsorbent by using centrifugation at the rotational speed of 4900 rpm for 10 min. The SG contents in PO-B100 before and after adsorption were analyzed using UV-mini 1240 spectrophotometer (Shimadzu, Japan) at 240 nm, according to the modified technique conducted by Moreau et al. (2008), Nystro€m (2007) and Araújo et al. (2013) [14,27,28]. The

24percentage of SG removal was determined by using the following equation

. SG removal ð%Þ ¼ Ci ? Cf x100 (2) Ci Where Ci is the concentration of SG in untreated PO-B100 (mg/kg) and Cf is

2the concentration of SG in treated (after adsorption) PO- B100

(mg/kg). The results of SG removal were verified by using GC-FID analysis (see section 2.4) and its statistical approach was performed using Minitab software (version 18.1) to identify the significance order of the parameters affecting the adsorption. 2.6. Isotherm and thermodynamics study of the SG adsorption The adsorption isotherm was conducted at the temperature of 65, 75 and 85 C with various CFP-based NCC to PO-B100 mass ratio (1:50, 1:75, 1:100, 1:125, 1:150, 1:175, 1:200). It was performed using a similar procedure as previously mentioned in subsection 2.5. At the equilibrium condition, the amount of adsorbed SG per unit mass of CFP-based NCC as the adsorbent (Qe) was calculated by the equation below. mg Qe g ¼ Co ? Ce x V m (3) Where Co

9and Ce are the initial and final (equilibrium) concentra- tion of SG in PO-B100 (mg/L), respectively, m is the mass of adsorbent (g) and V is the volume of PO-B100 (L). The

equilibrium data obtained at various temperature

6were fitted to the three isotherm models, namely Langmuir, Freundlich and Dubinin-Radushkevich (D-R). Meanwhile, the

thermodynamic

16parameters such as Gibbs free energy change (DG), enthalpy (DH) and entropy (DS) were further determined

from the results of isotherm study using equations (4) and (5). D G ¼ ? RTIn KL:MSG:103:Co (4) DG ¼DH ? TDS (5) Where

15**R is the gas constant** with the value **of 8.314 J**/mol.**K**, **T is the** absolute **temperature** in Kelvin, **KL is Langmuir**

equilibrium con- stant in L/mg, MSG is the molecular weight of SG in g/mol and Co is the reference concentration in standard state with the value of 1 mol/L.

13. Results and discussions 3.1. Characterization of CFP-based NCC The

27X-ray diffraction pattern of the CFP and its NCC are shown

in Fig. 1, and the corresponding crystallinity index is presented in Table 1. Both XRD patterns showed the cellulose I characteristic peaks at 2q around 15e17 (110 crystal plane) and 22e23 (200 crystal plane) [26,29]. The crystallinity index of CFP and its NCC were calculated using equation (1) and recorded to have the cor- responding value of 57.60% and 85.73%. The change of crystallinity has occurred

27because of the progressive removal of amorphous hemicellulose and lignin

during acid hydrolysis. The highly crys- talline product is more efficient to improve the mechanical properties of the composite material, particularly as an adsorbent, since crystallinity positively corresponds to the tensile strength of the material [30]. The scanning electron micrograph in Fig. 2 shows the shape and size of the CFP-based NCC. The distribution of NCC products derived from CFP was estimated to have approximately 200e400 nm in length (Fig. 2). The prepared CFP-based NCC has a homogenous needleshaped with crystallite size in the range of 2e4 nm, ob- tained from the combination of X-ray diffraction data and Scherrer analysis. The homogenous CFP-based NCC particles are likely caused by the swollen of cellulose fibers due to NaOH delignifica- tion pretreatment [25]. Fig. 3 (a) e (b) illustrated the FTIR spectra of CFP-based NCC before and after adsorption. As shown in Fig. 3 (a), several peaks representing certain functional groups in CFP-based NCC were found in the spectra. The broad

14band in the range of 3008e3459 cm?1 represents the

OeH stretching vibrations, while Fig. 1. X-ray diffraction patterns of (a) CFP, (b) CFP-based NCC. Table 1 The crystallinity index of CFP and CFP-based NCC. Samples 2-theta () Crystallinity (%) 110 crystal plane 200 crystal plane CFP 15.44 22.63 57.60 CFP-based NCC 16.52 22.60 85.73 Fig. 2. SEM image of the rodlike CFP-based NCC particles.

15Fig. 3. FTIR spectrum of (a) CFP-based NCC before adsorption and (b

) CFP-based NCC after adsorption.

14the peaks in the range of 2802e2925 cm?1 correspond to

21stretching vibrations. The absorption at 936e1137 cm?1 is related to the

functional group of CeOeC, and the peak at 1640 cm?1 in- dicates the

21presence of abundant hydrophilic hydroxide group in the cellulose

[31]. A peak at 1382 cm?1 represents the CeH asym- metric deformations [32]. Meanwhile, Fig. 3 (b) showed strong peaks in the wavenumbers of around 1019e1376 cm?1 and 2602e3160 cm?1, which represent the CeO moiety, and CH2 and CH3 stretching vibrations. These two specific peaks are known as the fingerprint areas for SG. Another

14peak at 1750 cm?1 corresponds to the typical C]O stretching band of the

methyl ester, while an OeH band around 3110 - 3700 cm?1 indicates the presence of hydroxyl groups in SG and CFP-based NCC [33]. Therefore, based on the FTIR

20spectra, it can be concluded that SG is the major component of the

adsorbate on the surface of CFP- based NCC, which is consistent with the GC-FID results discussed in section 3.2. 3.2. Properties of PO-B100 The properties of PO-B100 have been analyzed according to the standard method of ASTM for its content of FAME, acid value (AV), MG, DG and triglycerides (TG). As reported in Table 2, the purity of FAME in PO-B100 is 98.7%, while the AV, MG, DG, and TG values are 0.12 mg KOH/g, 0.23%, 0.09%, and 0.06%, respectively. Furthermore,

2PO-B100 feedstock contained 194.1 mg/kg of SG

with the cloud point of 13.2 C and a clear initial appearance. Based on the GC-FID analysis, the SG profile in PO-B100 consists of 34.79% of campes- teryl glucoside, 23.73% of stigmasteryl glucoside and 41.48% of b- sitosteryl glucoside. The results met the requirements of ASTM D6751 and SNI 7182:2015. However, white precipitates could be found within a few hours after production. After the adsorption using the parameters giving the highest SG removal (1:50, 75 C, 1 h; see section 3.3), the sample of treated PO-B100 was collected for the properties measurement

2in order to monitor the effect of the adsorbent

. According to the results, the

2treated PO-B100 contained FAME with a purity of

98.8% and AV

2value of 0.11 mg KOH/g

. The concentration of SG reduced signifi- cantly to 15.9 mg/kg with the composition of 24.81% campesteryl glucoside, 25.07% stigmasteryl glucoside and 50.12% b-sitosteryl glucoside, while the other glycerides components, MG, DG, and TG, were slightly decreased to 0.22%, 0.09%, 0.05%, respectively. The cloud point of the treated PO-B100 was also found to be decreased to 11.5 C. These results indicated that CFPbased NCC has selec- tivity to adsorb SG, particularly campesteryl glucoside and L. Widdyaningsih et al. / Renewable Energy 154 (2020) 99e106 103 Table 2 The properties of untreated and treated PO-B100 (1:50, 75 C, 1 h), and the comparison with ASTM D6751 and SNI 7182:2015. Parameters ASTM D6751 SNI 7182:2015 Untreated PO-B100 Treated PO-B100 (1:50, 75 C, 1 h) FAME (%) AV (mg KOH/g) MG (%) DG (%) TG (%) SG (mg/kg) Cloud point (C) 96.5 96.5 0.50 0.50 0.80 0.80 0.20 e 0.20 e N/Aa N/Aa e 18.0 98.7 0.12 0.23 0.09 0.06 194.1 13.2 98.8 0.11 0.22 0.09 0.05 15.9 11.5 a Not available. stigmasteryl glucoside, as compared to the other minor compo- nents, such as MG, DG, and TG. It also subsequently lowered the cloud point significantly, which is advantageous for storage and transportation purposes [34]. 3.3. Adsorption of SG using CFP-based NCC Fig. 4 summarized the SG removal rate at the various temper- ature and mass ratios of CFP-based NCC to PO-B100. The highest value of the SG removal rate (91.81%) was obtained at the following conditions: 75 C, CFP-based NCC to PO-B100 mass ratio of 1:50, and 1 h adsorption time. Based on the results

2shown in Fig. 4, the lowest removal rate of SG

in every adsorption temperature was seen at 1:200 of CFP-based NCC to PO-B100 mass ratio. It was likely due to insufficient binding and active adsorption sites and the adsorption required more time to reach the equilibrium stage. The

3removal percentage of SG was observed to have amplified

with the increase of CFP-based NCC to PO-B100 mass ratio from 1:200 to 1:50 at all temperatures in the tested range. Greater amounts of CFP-based NCC provide greater adsorption surface area and active sites in CFP-based NCC, leading to an adequate SG binding area and certainly, a higher percentage of SG removal [35]. It was also monitored that the SG removal rate exponentially increased when the CFP-based NCC to PO-B100 mass ratio was increased from 1:100 to 1:50 in the all adsorption temperature. The phenomenon indi- cated the good dispersion ability of CFP-based NCC in PO-B100, where constant diffusion path length of SG binding to CFP-based NCC surface was found regardless of the amount of adsorbent [36]. As depicted in Fig. 4, temperature also remarkably affected the SG reduction. A temperature elevation from 65 C to 75 C improves the reduction of SG, regardless of CFP-based NCC to PO-B100 mass ratio. Chowdhury et al. (2011) stated that the adsorption enhancement along with the temperature increase may be asso- ciated with the increase of the number of active sites available for adsorption. The diffusion rate of the adsorbate across the external boundary layer also escalates with the rise in temperature, due to lower solution viscosity and enhancement in the mobility and ki- netic energy of the adsorbate [37]. Therefore, the

4collision between particles intensifies with the temperature elevation so that the activation energy of the adsorption process is easier to achieve

. As a result, the amount of the adsorbed SG enhances along with the temperature increase. However, it was also observed that the SG removal rate

2decreased when the temperature was further esca- lated from 75 C to 85 C

. More (2018) mentioned that after reaching a certain temperature, excessive particle collision causes the removal of adsorbates from the adsorbent, leading to lower adsorption capacity [38]. Lee et al. (2019) also stated that the NCC surface binding generally weakens along with the temperature enhancement [36]. The fluctuations of the SG uptake observed with the change in temperature suggests that the SG adsorption is governed by both physical attraction and chemical bonding, indi- cating that the sorption of SG by CFP-based NCC is both driven by physical and chemical sorption [37,39]. Fig. 5 presented the

4Pareto chart of the standardized effect generated using statistical analysis (Minitab version 18.1). The

figure showed that both independent parameters (temperature and the mass ratio of CFP-based NCC to PO-B100) were

4found to be prominent with the significance order of

the mass ratio of CFP- based NCC to PO-B100 > temperature. The other quadratic and two-way interaction terms were also found to significantly affect the SG removal rate. 100 80 65°C 75°C 85°C SG removal (%) 60 40 20 0 1:200 1:175 1:150 1:125 1:100 1:75 1:50 Mass ratio of CFP-based NCC to PO-B100 Fig. 5. The Pareto chart of the standardized effect showing the significance order of the Fig. 4. SG removal rate varied with the mass ratio of CFP-based NCC to PO-B100 at two independent variables (temperature and mass ratio of NCC to PO-B100) on the SG three different temperatures. removal, generated by ANOVA. 3.4. Study of adsorption isotherm and thermodynamic parameters In this study, three isotherm equations

8were fitted to the experimental equilibrium data for SG at

three temperature points (65 C, 75 C and 85 C). The results are presented in Table 3 and the isotherm models are plotted in Fig. 6. The Langmuir isotherm constant, KL and maximum absorption capacity, Qm(L) were calcu- lated from the nonlinear curve fitting between Qe and Ce. The value of Qm(L) was found to be increased from 12.50 mg/g at 65 C to 12.93 mg/g at 75 C before declining to 11.24 mg/g at the highest tested temperature (85 C). The Qm(L) results are quite comparable to the adsorption capacity of magnesium silicate and bleaching earth on the SG (~13 mg/g) [16]. The

 $6Langmuir \ constant \ (KL) \ also \ increases \ along \ with \ the \ temperature, \ from \ 0.11 \ L/mg \ at$

the lowest temperature (65

6C) to 0.26 L/mg at

the highest temperature point (85 C), indicating that the adsorption of SG to CFP-based NCC is an endothermic

8process. The isotherm data were further analyzed by the Freundlich model.

The Freundlich constant KF and 1/n were obtained from the

non-linear regression analysis. Table 3 showed that the values of 1/ n are all under unity, ranging from 0.03 at 75 C to 0.16 at 65 C. The extent of 1/n represents the favorability degree of adsorption. The value of 1/n less than unity corresponds to favorable sorption. It was also observed that the Freundlich constant greatly escalates along with the temperature, implying that the adsorption was favorable at high temperature and the process is certainly endo- thermic. de Sa et al. (2017) mentioned that 1/n value between 0 and 1 is associated with a chemisorption process [40]. Another isotherm equation, the

9Dubinin-Radushkevich (D-R) model, was further applied to analyze the equilibrium data

, particularly to determine the nature of SG adsorption onto CFP- based NCC surface. The D-R

29constant (b) gives an idea about the mean sorption energy, E, and their correlation can be expressed by the following

2516 kJ/mol, the sorption process is supposed to be chemisorption, while for energy value lower than 8 kJ/mol, the sorption is of physical

nature [41,42].

5Based on the results provided in Table 3, the

adsorption mechanism is physical attraction since the E values for all tested temperatures are lower than 8 kJ/mol. The highest Qm(D-R) was found at 75 C with a value of 12.13 mg/g, which was similar to Table 3 Isotherm parameters of SG adsorption onto CFP-based NCC surface. Isotherm Parameters Temperature (K) 338 348 358 Langmuir Freundlich Dubinin-Radushkevich Qm(L) (

22mg/g) KL (L/mg) r2 c2 KF ((mg/g) (L/mg)1/n) 1/n r2 c2 Qm(D-R) (mg/g

) E (kJ/mol) r2 c2 12.50 12.93 0.11 0.16 0.8587 0.8580 0.2329 0.2865 5.59 6.48 0.16 0.03 0.8408 0.7986 0.2624 0.4064 11.58 12.13 0.18 0.25 0.8094 0.8387 0.3147 0.3254 11.24 0.26 0.7039 0.2487 7.31 0.09 0.6079 0.3293 10.86 0.29 0.7555 0.2053 14 12 Qe (mg/g) 10 Langmuir Freundlich Dubinin-Radushkevich (D-R) 8 0 50 100 Ce (mg/L) Fig. 6. The modelled isotherm profiles for the adsorption of SG to CFP-based NCC surface (temperature 75 C, mass ratio of CFP-based NCC to PO-B100 1:50, ¼ ¼ time ¼ 1 h, agitation speed ¼ 250 rpm). the result obtained using Langmuir isotherm. The effect of tem- perature previously

studied also provides similar results where the temperature of 75 C gives the highest SG removal rate compared to the other tested temperatures. The

8correlation coefficient (r2) and chi-square (c2) values of the three isotherms are also listed

17in Table 3. It could be concluded that the adsorption of SG onto

the CFP-based NCC surface is

17best fitted to the Langmuir isotherm equation under the temperature range studied. Based on the

three isotherm models studied, the adsorp- tion mechanism is predicted to be driven by both physical and chemical sorption due to its sorption energy value and endo- thermic nature, respectively. The overall results of this study showed that NCC has a particular affinity for SG and is an effective adsorbent for SG removal from PO-B100. Table 4 listed the thermodynamics parameters of the SG adsorption onto the surface of NCC,

16such as Gibbs free energy change (DG), enthalpy (DH) and entropy (DS

). The values of Gibbs free energy (DG) for the adsorption of SG were negative at all tested temperatures. These values confirm the spontaneous nature of SG adsorption onto the CFP-based NCC. Enhancement of the DG value along with the increasing temperature implies

9that the affinity of SG on CFP-based NCC was higher at high tempera- ture. Positive DH value

(42.90 kJ/mol) verifies that the adsorption is indeed an endothermic process, while the absolute value of D S (219.80 J/mol.K) reflects the increased randomness at the solid- solution interface during the adsorption process [37,43]. 3.5. Adsorption mechanism study The study of the adsorption mechanism was used to further illustrate the interaction between SG and CFP-based NCC surface. Two important points have to be considered to understand the

24Table 4 Thermodynamic parameters of adsorption of SG onto

CFP-based NCC surface.

6Temperature (K) Thermodynamic parameters DG (kJ/mol) DH (kJ/mol) DS (J/mol.K

) 338 348 358 ?31.44 ?33.46 ?35.84 42.90 219.80 L. Widdyaningsih et al. / Renewable Energy 154 (2020) 99e106 105 mechanism, namely the

3surface properties of the adsorbent and the structure of adsorbate. The

NCC molecule was constructed by a substantial

23number of hydrogen bonds between glucose units or glucose chains inside the molecule to form a very stable structure

[44,45]. NCC contains the majority of oxygen functional groups such as hydroxyl, ether, and sulfonate. While the hydroxyl and ether groups are originally present in the cellulosic material, the sulfonate group existed due to the acid hydrolysis to produce NCC. On the other hand, SG was built by a steryl cation (SCb) and a glucose unit, with a positive charge on the cationic steryl part. According to the findings of this study, the adsorption was temperature-dependent and the isotherm modeling showed an equal contribution of physical attraction and chemical binding. Therefore, the mechanism of SG removal by adsorption on the CFP- based NCC surface

26may be presumed to involve these following steps: Migration of SG from the bulk of PO-B100 to the CFP-based NCC surface Diffusion of SG through the

8boundary layer to the CFP-based NCC surface Adsorption of SG on the surface of

CFP-based NCC, which may be caused by physical interaction of dipole-dipole coupling be- tween the positively charged SCb and the negatively charged NCC surface as suggested in Fig. 7; and through a possible chemical binding mechanism of ion exchange as shown below: NCC ? OH4NCC ? O? b Hb NCC ? SO?34NCC ? SO?3 NCC ? O? b SCb4NCC ? O ? SC NCC ? OH4NCC ? O? b Hb Intraparticle diffusion of SG into the pores of CFP-based NCC OH- SO3- OH- SO3- Nanocrystalline cellulose SO3- OH O HO HO OH OH- O3S -HO dipole-dipole coupling NCC surface sc+ O Fig. 7. Schematic representation of the proposed adsorption mechanism of SG onto CFP-based NCC surface. 4. Conclusions CFP-based NCC was successfully used as an adsorbent for reducing SG in PO-B100. The content of SG was able to be reduced from 194.1

2mg/kg to as low as 15.9 mg/kg

(91.81% removal rate) within 1 h at the temperature of 75 C using CFP-based NCC to PO- B100 mass ratio of 1:50. The study proved that CFP-based NCC has great affinity and selectivity to SG, particularly on the campesteryl glucoside and stigmasteryl glucoside. The adsorption treatment greatly improves the cold stability of PO-B100 by reducing the cloud point from 13.2 C to 11.5 C, while slightly affected the purity of FAME, AV and other minor components, such as MG, DG, and TG, which were still

2in the acceptable range according to ASTM D6751. The adsorption

process was endothermic and may be driven by both physical attraction and chemical ion exchange. The adsorption treatment using CFP-based NCC

2should be a prospective method used to remove SG from

PO-B100 since it possesses high efficiency, time-saving and energy-efficient.

10Declaration of competing interest The authors declare that they have no known competing financial interests or personal relationships that could have appeared to influence the work reported in this paper. CRediT authorship contribution statement Liangna Widdyaningsih: Conceptualization, Methodology, Investigation, Software, Writing - original draft

. Albert Setiawan:

7Conceptualization, Methodology, Investigation, Software, Writing - original draft. Shella Permatasari Santoso: Conceptualization, Data curation, Supervision. Felycia Edi Soetaredjo: Resources, Visualization

. Suryadi Ismadji: Resources, Validation. Sandy Budi Hartono:

1Software, Validation. Yi-Hsu Ju: Writing - review & editing. Phuong Lan Tran-Nguyen: Writing - review editing

. &

7Maria Yuliana: Conceptualization, Resources, Visualization, Writing - review & editing, Supervision

. Acknowledgment

28**This work was supported by Widya Mandala Catholic University** Surabaya, Indonesia, **through research grant no**. 0675/**WM01/N**

/ 2019. References [1] N. Kumar, A. Sonthalia, H.S. Pali, Sidharth, Alternative Fuels for Diesel Engines: New Frontiers, Diesel Engines [Working Title], 2018, pp. 1e27, https://doi.org/ 10.5772/intechopen.80614. [2] A.C. Pinto, L.L.N. Guarieiro, M.J.C. Rezende, N.M. Ribeiro, A. Ednildo, Biodiesel : An Overview, 16, 2005, pp. 1313e1330. [3] Z. Qiu, L. Zhao, L. Weatherley, Process intensification technologies in contin- uous biodiesel production, Chem. Eng. Process. Process Intensif. 49 (2010) 323e330, https://doi.org/10.1016/j.cep.2010.03.005. [4] Y.H. Ju, L.H. Huynh, Y.A. Tsigie, Q.P. Ho, Synthesis of biodiesel in subcritical water and methanol, Fuel 105 (2013) 266e271, https://doi.org/10.1016/j.fuel.2012.05.061. [5] S. Thiruvenkadam, S. Izhar, Y. Hiroyuki, R. Harun, One-step microalgal bio- diesel

production from Chlorella pyrenoidosa using subcritical methanol extraction (SCM) technology, Biomass Bioenergy 120 (2019) 265e272, https:// doi.org/10.1016/j.biombioe.2018.11.037. [6] F.H. Santosa, L. Laysandra, F.E. Soetaredjo, S.P. Santoso, S. Ismadji, M. Yuliana, A facile noncatalytic methyl ester production from waste chicken tallow using single step subcritical methanol: optimization study, Int. J. Energy Res. 43 (2019) 8852e8863, https://doi.org/10.1002/er.4844. [7] M. Aghilinategh, M. Barati, M. Hamadanian, Supercritical methanol for one put biodiesel production from chlorella vulgaris microalgae in the presence of CaO/TiO 2 nano-photocatalyst and subcritical water, Biomass Bioenergy 123 (2019) 34e40, https://doi.org/10.1016/j.biombioe.2019.02.011. [8] L.K. Ong, C. Effendi, A. Kurniawan, C.X. Lin, X.S. Zhao, S. Ismadji, Optimization of catalyst-free production of biodiesel from Ceiba pentandra (kapok) oil with high free fatty acid contents, Energy 57 (2013) 615e623, https://doi.org/ 10.1016/i.energy.2013.05.069, [9] M.K. Lam, K.T. Lee, A.R. Mohamed, Homogeneous, heterogeneous and enzy- matic catalysis for transesterification of high free fatty acid oil (waste cooking oil) to biodiesel: a review, Biotechnol. Adv. 28 (2010) 500e518, https:// doi.org/10.1016/j.biotechadv.2010.03.002. [10] L.P. Christopher, Hemanathan Kumar, V.P. Zambare, Enzymatic biodiesel: challenges and opportunities, Appl. Energy 119 (2014) 497e520, https:// doi.org/10.1016/j.apenergy.2014.01.017. [11] B. Likozar, A. Pohar, J. Levec, Transesterification of oil to biodiesel in a continuous tubular reactor with static mixers: modelling reaction kinetics, mass transfer, scale-up and optimization considering fatty acid composition, Fuel Process. Technol. 142 (2016) 326e336, https://doi.org/10.1016/ j.fuproc.2015.10.035. [12] I. Lee, L.M. Pfalzgraf, G.B. Poppe, E. Powers, T. Haines, The role of sterol glu- cosides on filter plugging, Biodiesel Mag 4 (2007) 105e112. [13] V. Van Hoed, N. Zyaykina, W. De Greyt, J. Maes, R. Verhe, K. Demeestere, Identification and occurrence of steryl glucosides in palm and soy biodiesel, JAOCS, J. Am. Oil Chem. Soc. 85 (2008) 701e709, https://doi.org/10.1007/ s11746-008-1263-5. [14] R.A. Moreau, K.M. Scott, M.J. Haas, The identification and quantification of steryl glucosides in precipitates from commercial biodiesel, JAOCS, J. Am. Oil Chem. Soc. 85 (2008) 761e770, https://doi.org/10.1007/s11746-008-1264-4. [15] H. Tang, S.O. Salley, K.Y. Simon Ng, Fuel properties and precipitate formation at low temperature in soy-, cottonseed-, and poultry fat-based biodiesel blends, Fuel 87 (2008) 3006e3017, https://doi.org/10.1016/j.fuel.2008.04.030. [16] D. Na-Ranong, P. Laungthaleongpong, S. Khambung, Removal of steryl glu- cosides in palm oil based biodiesel using magnesium silicate and bleaching earth, Fuel 143 (2015) 229e235, https://doi.org/10.1016/j.fuel.2014.11.049. [17] A. Aguirre, S. Peiru, F. Eberhardt, L. Vetcher, R. Cabrera, H.G. Menzella, Enzy- matic hydrolysis of steryl glucosides. major contaminants of vegetable oil- derived biodiesel, Appl. Microbiol. Biotechnol. 98 (2014) 4033e4040, https://doi.org/10.1007/s00253-013-5345-4. [18] S. Peiru, A. Aguirre, F. Eberhardt, M. Braia, R. Cabrera, H.G. Menzella, An in- dustrial scale process for the enzymatic removal of steryl glucosides from biodiesel, Biotechnol. Biofuels 8 (2015), https://doi.org/10.1186/s13068-015- 0405-x. [19] A.Y. Tremblay, A. Montpetit, The in-process removal of sterol glycosides by ultrafiltration in biodiesel production, Biofuel Res. J. 4 (2017) 559e564, https://doi.org/10.18331/brj2017.4.1.6. [20] M.Y. Chang, R.S. Juang, Adsorption of tannic acid, humic acid, and dyes from water using the composite of chitosan and activated clay, J. Colloid Interface Sci. 278 (2004) 18e25, https://doi.org/10.1016/j.jcis.2004.05.029. [21] A.G. Varghese, S.A. Paul, M.S. Latha, Green Adsorbents for Pollutant Removal, 2018, https://doi.org/10.1007/978-3-319-92111-2. [22] M. Bo€rjesson, G. Westman, Crystalline nanocellulose d preparation, modifi- cation, and properties, Cellul. -Fundam. Asp. Curr. Trends. (2015), https:// doi.org/10.5772/61899. [23] H. Voisin, L. Bergstro€m, P. Liu, A. Mathew, Nanocellulose-based materials for water purification, Nanomaterials 7 (2017) 57, https://doi.org/10.3390/ nano7030057. [24] H. Liang, X. Hu, A quick review of the applications of nano crystalline cellulose in wastewater treatment, J. Bioresour. Bioprod. (2016) 199e204, 2016, www. Bioresources-Bioproducts.com. [25] J.N. Putro, S.P. Santoso, S. Ismadji, Y.H. Ju, Investigation of heavy metal adsorption in binary system by nanocrystalline cellulose e bentonite nano- composite: improvement on extended Langmuir isotherm model, Micropo- rous Mesoporous Mater. 246 (2017) 166e177, https://doi.org/10.1016/ j.micromeso.2017.03.032. [26] L. Segal, J.J. Creely, A.E. Martin, C.M. Conrad, An empirical method for esti- mating the degree of crystallinity of native cellulose using the X-ray diffractometer, Textil. Res. J. 29 (1959) 786e794, https://doi.org/10.1177/ 004051755902901003. [27] L. Nystro€m, Occurrence and Properties of Steryl Ferulates and Glycosides in Wheat and Rye, University of Helsinki, 2007. [28] L.B.D.C. Araújo, S.L. Silva, M.A.M. Galva~o, M.R.A. Ferreira, E.L. Araújo, K.P. Randau, L.A.L.

Soares, Total phytosterol content in drug materials and extracts from roots of Acanthospermum hispidum by UV-VIS spectropho- tometry, Brazilian J. Pharmacogn. 23 (2013) 736e742, https://doi.org/ 10.1590/S0102-695X2013000500004. [29] M.N.A.M. Taib, W.A. Yehye, N.M. Julkapli, Influence of crosslinking density on antioxidant nanocellulose in bio-degradation and mechanical properties of nitrile rubber composites, Fibers Polym. 20 (2019) 165e176, https://doi.org/ 10.1007/s12221-019-8575-y. [30] Y. Hu, L. Tang, Q. Lu, S. Wang, X. Chen, B. Huang, Preparation of cellulose nanocrystals and carboxylated cellulose nanocrystals from borer powder of bamboo, Cellulose 21 (2014) 1611e1618, https://doi.org/10.1007/s10570-014-0236-0. [31] A. Alemdar, M. Sain, Isolation and characterization of nanofibers from agri- cultural residues - wheat straw and soy hulls, Bioresour. Technol. 99 (2008) 1664e1671, https://doi.org/10.1016/j.biortech.2007.04.029. [32] X.F. Sun, F. Xu, R.C. Sun, P. Fowler, M.S. Baird, Characteristics of degraded cellulose obtained from steamexploded wheat straw, Carbohydr. Res. 340 (2005) 97e106, https://doi.org/10.1016/j.carres.2004.10.022. [33] H. Wang, H. Tang, S. Salley, K.Y. Simon Ng, Analysis of sterol glycosides in biodiesel and biodiesel precipitates, JAOCS, J. Am. Oil Chem. Soc. 87 (2010) 215e221, https://doi.org/10.1007/s11746-009-1489-x. [34] N.A. Negm, M.T.H. Abou Kana, M.A. Youssif, M.Y. Mohamed, Biofuels from Vegetable Oils as Alternative Fuels: Advantages and disadvantages, 2017, https://doi.org/10.1201/b20780. [35] A. Khodabandehloo, A. Rahbar-Kelishami, H. Shayesteh, Methylene blue removal using Salix babylonica (Weeping willow) leaves powder as a low-cost biosorbent in batch mode: kinetic, equilibrium, and thermodynamic studies, J. Mol. Lig. 244 (2017) 540e548, https://doi.org/10.1016/j.mollig.2017.08.108. [36] H.J. Lee, H.S. Lee, J. Seo, Y.H. Kang, W. Kim, T.H.K. Kang, State-of-the-art of cellulose nanocrystals and optimal method for their dispersion for construction-related applications, Appl. Sci. 9 (2019) 1e14, https://doi.org/ 10.3390/app9030426. [37] S. Chowdhury, R. Mishra, P. Saha, P. Kushwaha, Adsorption thermodynamics, kinetics and isosteric heat of adsorption of malachite green onto chemically modified rice husk, Desalination 265 (2011) 159e168, https://doi.org/ 10.1016/j.desal.2010.07.047. [38] H. More, Factors Affecting Adsorption. https://hemantmore.org.in/science/ chemistry/factors-affecting-adsorption/13094/, 2018 accessed May 5, 2019. [39] M. Mohapatra, S. Khatun, S. Anand, Kinetics and thermodynamics of lead (II) adsorption on lateritic nickel ores of Indian origin, Chem. Eng. J. 155 (2009) 184e190, https://doi.org/10.1016/j.cej.2009.07.035. [40] A. de Sa, A.S. Abreu, I. Moura, A.V. Machado, Polymeric Materials for Metal Sorption from Hydric Resources, Elsevier Inc., 2017, https://doi.org/10.1016/ b978-0-12-804300-4.00008-3. [41] C.S. Zhu, L.P. Wang, W. bin Chen, Removal of Cu(II) from agueous solution by agricultural by-product: peanut hull, J. Hazard Mater. 168 (2009) 739e746, https://doi.org/10.1016/j.jhazmat.2009.02.085. [42] Q. Li, L. Chai, Z. Yang, Q. Wang, Kinetics and thermodynamics of Pb(II) adsorption onto modified spent grain from aqueous solutions, Appl. Surf. Sci. 255 (2009) 4298e4303, https://doi.org/10.1016/j.apsusc.2008.11.024. [43] Y. Liu, Y.J. Liu, Biosorption isotherms, kinetics and thermodynamics, Separ. Purif. Technol. 61 (2008) 229e242, https://doi.org/10.1016/ j.seppur.2007.10.002. [44] Y. Habibi, L.A. Lucia, O.J. Rojas, Cellulose nanocrystals: chemistry, selfassembly, and applications, Chem. Rev. 110 (2010) 3479e3500, https://doi.org/10.1021/cr900339w. [45] Y. Liu, D. Ying, L. Sanguansri, Y. Cai, X. Le, Adsorption of catechin onto cellulose and its mechanism study: kinetic models, characterization and molecular simulation, Food Res. Int. 112 (2018) 225e232, https://doi.org/10.1016/ j.foodres.2018.06.044. 100 L. Widdyaningsih et al. / Renewable Energy 154 (2020) 99e106 102 L. Widdyaningsih et al. / Renewable Energy 154 (2020) 99e106 104 L. Widdyaningsih et al. / Renewable Energy 154 (2020) 99e106 106 L. Widdyaningsih et al. / Renewable Energy 154 (2020) 99e106